BMC Plant Biology

RESEARCH Open Access

Unveiling resistance expression profile to powdery mildew in wheat via Bulked Segregant RNA-Seq

Tianying Yu[1*], Shengliang Cao[1], Yuli Jin[1], Chunxia Xu[1], Ruobing Liu[1], Bo Wang[1], Yue Lv[1], Ting Meng[1] and Pengtao Ma[1*]

Abstract

Background Developing wheat cultivars with durable resistance to powdery mildew, caused by *Blumeria graminis* f. sp. *tritici* (*Bgt*), is crucial for sustainable agriculture. The wheat genotype MYC exhibited high resistance to the *Bgt* isolate E09 at the seedling stage. Genetic analysis identified a recessive gene, temporarily named *PmMYC*, responsible for this resistance. Understanding the molecular mechanisms underlying this resistance is essential for advancing breeding programs.

Results Bulked Segregant RNA-Seq revealed numerous alternative splicing events generated following *Bgt* infection, suggesting powdery mildew may disrupt alternative splicing and affect immune responses. Gene Ontology (GO) analysis indicated significant enrichment of differentially expressed genes in "response to stimuli" and "immune system processes", implying their roles in disease defense. BSR-Seq analysis identified two high-confidence candidate regions for *PmMYC* on chromosome 2B, spanning 40,451,950 – 102,426,703 bp and 421,707,046–449,840,516 bp. Within these intervals, 740 genes were identified, with nonsynonymous mutations in 46 genes in the parents and bulks. Real-time PCR showed distinct expression profiles in four genes in resistant MYC compared to susceptible Yannong 21. KEGG and COG analyses of differentially expressed genes in candidate intervals revealed enrichment in immune processes related to plant-pathogen interactions, confirming that *PmMYC* initiated a broad immune response to prevent *Bgt* invasion.

Conclusion The study identified key genetic intervals and genes involved in the resistance of wheat genotype MYC to *Bgt*. The identified genes, particularly those with altered expression profiles, could serve as valuable targets for breeding programs aimed at developing wheat cultivars with durable resistance to powdery mildew. These findings enhanced our understanding of plant-pathogen interactions and provided a foundation for future genetic and functional studies.

Keywords *Triticum aestivum* L., Powdery mildew, *PmMYC*, BSR

*Correspondence:
Tianying Yu
tyyu@ytu.edu.cn
Pengtao Ma
ptma@ytu.edu.cn
[1]College of Life Sciences, Yantai University, Yantai 264005, China

Introduction

Common wheat (*Triticum aestivum* L.) is one of the most important cereal crops globally, providing a quarter to a fifth of food nutrition and feeding half of the world's population (FAO, 2017). In wheat production, powdery mildew, caused by the fungus *Blumeria graminis* f. sp. *tritici* (*Bgt*), is one of the most destructive diseases. Once infected, wheat yield will reduce from 5 to 40% in different countries [1]. In recent years, it has become widespread across almost all wheat-producing regions worldwide, especially in ones with humid or maritime climates [2]. In the present stage, the prevention and control measures of wheat powdery mildew mainly include cultivating resistant host cultivars, altering cultivation methods, and using chemical fungicides [3]. Compared to the latter two measures, cultivating host-resistant cultivars is the most fundamental, economical, effective, and environment-friendly strategy for controlling this disease [4].

Plants face constant threats from various pathogens [5]. Unlike acquired immunity in animals, plants evolve and develop innate immune systems to combat pathogenic threats [6]. The innate immune system of plants comprises two layers: pathogen-associated molecular pattern (PAMP)-triggered immunity (PTI) and effector-triggered immunity (ETI). Firstly, cell surface-located pattern recognition receptors (PRRs) recognize PAMP to trigger PTI, which functions as the first layer of the plant's innate immune system [7]. However, many pathogens have evolved the ability to inject virulent effectors into host cells. This suppresses or interferes with the PTI response of the host immune system, leading to more effective infection and colonization. Accordingly, host cells have evolved to produce a variety of intracellular immune receptors, known as NLRs (Nucleotide-binding domain and Leucine-rich repeat Receptors). These receptors detect effectors and initiate the secondary layers of defense, referred to as ETI [3], which trigger local hypersensitive reactions (HR), leading to programmed cell death. This limits the spread of infection, enhancing PTI and ETI [8]. The crosstalk between ETI and PTI amplifies and collaborates to produce a sustainable and intensive immune response to combat pathogen invasion [8–10]. Plants and pathogens have engaged in a fierce "arms race". Plants establish the first barrier to defense against the invasion of pathogens through PPRs [11]. Accordingly, pathogens develop effectors to bypass the defense line and directly enter the plant cells. This adaptive evolution of pathogens may exert selective pressure on plants. To combat such threats, plants have evolved NLRs, also known as resistance genes (R genes), which directly or indirectly recognize effectors. This recognition triggers hypersensitive responses, leading to localized cell death and preventing the spread of infection. This relationship of mutual adaptability promotes the co-evolution between the interacting species [3]. Long-term co-evolution of plants and pathogens would drive the molecular evolution of genes involved in the interaction between pathogen and host, such as effectors and R genes. Most plant R genes prefer to be in recombination hotspots in wheat and Tomato [12, 13]. The large gene families lain in complex clusters of paralogous genes undergo rapid evolution through rearrangement and recombination, resulting in novel and specific R genes.

Clear genomic information is a prerequisite for dissecting the genetic and molecular mechanisms underlying resistance to wheat powdery mildew. However, the genome of common wheat is enormous and intricate. It is an allohexaploid (2n=6x=42; AABBDD) genome structure derived from two polyploidization events. Tetraploid wheat (*Triticum turgidum*; 2n=4x=28; AABB) originated from the hybridization between wild diploid wheat (*Triticum urartu*; A subgenome donor) and a close relative of *Aegilops speltoides* (B subgenome donor) [14]. Subsequently, hexaploid wheat (AABBDD) originated through the hybridization of tetraploid wheat (AABB) with diploid *Aegilops tauschii*, which provided the D subgenome [14]. PRR and R genes form large gene families with members presented in all three homologous A, B, and D genomes in hexaploid common wheat. The resistance of wheat to powdery mildew possesses two kinds of models: qualitative and quantitative. Among them, the qualitative resistant genes abide by Mendelian's inheritance law. Even if it is a qualitative resistant gene, each allele in the same loci produces different resistance to different pathogenic races; for instance, *Pm3a*, *Pm3b*, *Pm3c*, *Pm3d*, *Pm3e*, and *Pm3f* recognize *AvrPm3* derived from different specific isolate races [15–17]. The qualitative resistant genes are race-specific and tend to progressively compromise as new races of wheat powdery mildew emerge in the field.

Furthermore, domestication and intensive breeding have reduced the diversity of the wheat germplasm resources. With the implementation of various control strategies, the selective pressure of powdery mildew increased, forcing it to speed up the establishment of adaptability. All these make it easy for resistant cultivated cultivars to lose their effectiveness against wheat powdery mildew. Based on the analysis and in-depth understanding of the molecular mechanism of the interaction underlying wheat and powdery mildew, pyramiding diverse and various types of resistant genes to breed broad-spectrum and durable resistant cultivars, is the most effective strategy against wheat powdery mildew. To discover new resistant genes and increase genetic diversity, wheat landrace-resistant cultivars against powdery mildew have been studied.

The common wheat cultivar MYC exhibits significant resistance to powdery mildew at the seedling stage. This study aims to elucidate the genetic and molecular mechanisms underlying this resistance by (1) characterizing the genetic basis using a recombinant inbred population derived from the resistant MYC and susceptible cultivar Yannong 21 (YN21); (2) employing an integrated Bulked Segregant Analysis (BSA) and RNA sequencing (BSR) strategy to uncover differential expression profiles associated with MYC resistance on a global genomic scale; (3) identifying candidate genomic intervals for the *PmMYC* locus; and (4) detecting key genes linked to powdery mildew resistance. This research establishes a foundation for fine mapping and exploring molecular mechanisms in candidate genes, providing potential targets for the molecular breeding of wheat cultivars with durable resistance to powdery mildew.

Materials and methods

Plant materials

MYC, as the maternal parent, was crossed with the powdery mildew-susceptible cultivar YN21 (paternal parent) to generate F_1, F_2, and $F_{2:3}$ generations. This was done to assess the inheritance of powdery mildew resistance in progeny. As mentioned in previous studies, the wheat cultivar Huixianhong was used as the susceptible control [18].

Assessment of resistance to wheat powdery mildew

To observe the infection process, seedlings of MYC and YN21 were inoculated with *Bgt* isolate E09 at the two-leaf stage. As previously described, leaves from YN21 and MYC were sampled and stained with Coomassie Brilliant Blue at one, two, and three days post-inoculation (dpi) [19]. Bright-field images were captured using a ZEISS Axioscope 5 (ZEISS, Germany). The biomass ratio assay was executed at pre-infection as well as at each time point (1 dpi through 7 dpi), following established protocols [20]. Significance analysis was performed using a 2-way ANOVA test conducted via GraphPad Prism version 8.

To analyze the inheritance of powdery mildew resistance, MYC, YN21, and their derived F_1, F_2, and $F_{2:3}$ generations were inoculated with the *Bgt* isolate E09 using established dusting methods [21]. The phenotype and genotype of $F_{2:3}$ families from F2 plants were assessed to confirm genotypes. Infected seedlings were maintained in 100% humidity in a dark chamber at 18 °C for 24 h, then grown in a greenhouse with 90% relative humidity, a 12 h/12 h light/dark cycle, and temperatures of 18 °C/22°C (day/night). Approximately 7–10 dpi, once disease symptoms appeared on the first leaf of the susceptible control Huixianhong, infection types (ITs) were recorded using a 0–4 scale [18, 22, 23]. Seedlings with ITs of 0–2 were scored as resistant, and those with ITs of 3–4 were scored as susceptible. The disease phenotype was analyzed three times. At 14 dpi, the F_2 population from MYC and YN21, along with two bulks each of 30 $F_{2:3}$ families homozygous for resistance or susceptibility, were used for BSA-seq analysis.

Library construction, RNA sequencing, and alignment

Experiments were conducted following the standard procedures at Beijing Biomics Technology Co. Ltd. (Beijing, China). Total RNA was extracted from all four samples to assess RNA integrity. mRNA was isolated from the total RNA using Oligo (dT) magnetic beads paired with poly (A) tails. The mRNA was randomly fragmented with a fragmentation buffer. cDNA was synthesized from the mRNA template using six-base random primers (random hexamers) following the PrimeScript™ RT reagent Kit manual (TaKaRa, Japan). After cDNA purification and end repair, multiple adenine nucleotides were added at the 3'-terminus to form an A-tail. Then, sequencing adapters were ligated, followed by fragment size selection and PCR amplification. The cDNA library was constructed and its quality was rigorously examined. High-throughput sequencing was performed on the Illumina HiSeqTM 4000 platform (Illumina, USA).

Clean reads were obtained by filtering raw reads and removing adapters and low-quality reads. Quality scores of 30 (Q30, indicating detection accuracy > 99.9%) and GC contents of the clean reads were recorded. The clean reads were aligned to the Chinese Spring 2.1 reference genome using HISAT2 (v2.1.0) software (http://daehwankimlab.github.io/hisat2/download/). Mapped reads were assembled with StringTie (v2.1.5) software (https://ccb.jhu.edu/software/stringtie/index.shtml) following the reference genome-based method. The transcriptome data from the parent plants totaled 10.0 GB, while the data from the resistant and susceptible bulks exceeded 20.0 GB. These data were analyzed for SNP calling, BSR correlation, Gene Ontology (GO) [24] enrichment, Cluster of Orthologous Groups (COG) [25, 26] classification, and Kyoto Encyclopedia of Genes and Genomes (KEGG) [27] pathway analysis.

SNP (InDel) annotation

Sequence alignment was performed using the GATK (v3.1-1) software suite to identify potential SNPs. We compared transcriptome data from four samples against the reference genomes [28]. InDel (insertion/deletion), referring to insertions or deletions of small DNA segments, were analyzed relative to the reference genome The criteria for SNP (InDel) recognition were as follows: (1) No more than three consecutive single-base mismatches occurred within a 35 bp window; (2) The quality score for each SNP or InDel exceeded 2.0. SNPs (InDels)

were identified based on the annotation of the reference genome. Variants in susceptible bulks derived from resistant parents were filtered out if they had read support less than 4, multiple genotypes, or identical genotypes between resistant and susceptible bulks. High-confidence SNP (InDel) sites were then compiled. We analyzed their distribution across genomic regions (intergenic, genic, coding sequences, etc.). The types and frequencies of SNPs, including synonymous and non-synonymous mutations, were quantified.

BSR-seq analysis

The BSR-seq data analysis used the SNP-index and Euclidean distance (ED) method. The ED value of each SNP with significant differences in genotype between resistant and susceptible bulks was dotted.

(1) Calculation of ED: The ED value of each SNP was calculated according to the formula as follows:

$$ED = \sqrt{(A_R - A_S)^2 + (C_R - C_S)^2 + (G_R - G_S)^2 + (T_R - T_S)^2}$$

(R: resistant bulks, S: susceptible bulks).

Allele depths were normalization for both resistant and susceptible bulks. The ED value for each locus was calculated. The 5th power of the original ED was set as the correlation value to effectively eliminate background noise, followed by utilizing the SNPNUM approach to fit the ED value [29]. A threshold of 0.03 (median + 3SD) was set to identify significant loci.

(2) Calculation of the Δ(SNP-index): The following listed the formula of the Δ(SNP-index) using the ΔSNP-index correlation approach [42].

$$SNP_R - index = AD_R / (AD_R + AD_S), SNP_S - index = AD_S / (AD_R + AD_S)$$
$$\Delta(SNP - index) = SNP_R - index - SNP_S - index$$

(*AD*: Average depth, *R*: resistant bulks, *S*: susceptible bulks)

To calculate the SNP-index values in resistant and susceptible bulks, we used the MutMap approach, referencing SNPs from susceptible parents [30]. A sliding window method with a 5 Mb window size was employed to assess variations. We calculated the average ΔSNP-index across all chromosomes. The SNP screening threshold was set at 100,000 permutations with a 99% high confidence level. Candidate intervals with high confidence (> 99.0%) and ΔSNP-index values (> 0.75) were identified as associated with resistance to powdery mildew.

Identification and statistics of DEGs

After mapping and assembling, transcript expression levels were quantified using FPKM (Fragments Per Kilobase of transcript per Million fragments mapped) [29]. DEG was identified using the DESeq2 R package [31]. Screening criteria included an FDR (error detection rate) < 0.01 and a Fold Change (FC) ≥ 2. The statistical significance of DEGs was determined using multiple tests, with FDR adjusted by the Benjamini-Hochberg procedure [32].

Functional annotation and enrichment analysis

Differentially expressed genes were submitted to the IWGSC database (http://www.WheatGenome.org/, Wheat reference Genome RefSeq v2.1) for functional annotation. Gene Ontology [24], Cluster of Orthologous Groups [25, 26], and KEGG [27] pathways enrichment analyses were performed using the clusterProfiler R package [33]. The significance for GO and KEGG pathway enrichment was set at $p < 0.05$.

Alternative splicing event prediction

Alternative splicing (AS) transcripts were assembled using StringTie (v2.1.5) software (https://ccb.jhu.edu/software/StringTie/), based on Hisat2 (v2.1.0) software (http://daehwankimlab.github.io/hisat2/download/) mapped results against the reference genome. We employed ASprofile.b-1.0.4 to predict AS events and quantify expression levels for each sample (https://ccb.jhu.edu/software/ASprofile/). Statistical analyses were conducted on the types and number of AS events identified in both parental lines, as well as in the resistant and susceptible bulks.

Real-time PCR

The seedlings of MYC and YN21 were inoculated with fresh conidiospores of *Bgt* isolate E09 at the two-leaf stage. Total RNA was extracted from the inoculated leaves at various time points (0, 3, 6, 12, 24, 36, 48, and 72) hpi using an RNAprep Pure Plant Kit (Tiangen, China), following the manual of the manufacturer. RNA quality and concentration were assessed using a NanoDrop 1000 spectrophotometer (Thermo Fisher Scientific, USA). Genomic DNA was removed, and cDNA was synthesized using the TakaRa SuperScript kit (TakaRa, Japan) following the manufacturer's protocol. RT-PCR was conducted with SYBR Green as the double-stranded DNA-specific fluorescent dye (Tiangen, China) on a Rotor-Gene QPCR instrument (Applied Biosystems, USA) and repeated in triplicate. β-Tubulin was used as a reference gene, and relative mRNA expression levels were calculated using the 2^-ΔΔCT method. GraphPad Prism 8 software was utilized to generate group graphs, and significance analysis was performed using a 2-way ANOVA test conducted via GraphPad Prism.

Result

Identification of wheat powdery mildew resistance in MYC

On the leaf of MYC infected with *Bgt* E09 at 1–2 dpi, the development of fungal conidia was inhibited (Fig. 1.A a-b). However, conidia attached to the leaf surface, and formed two germ tubes: the primary germ tube and the appressorial germ tube (Fig. 1.A d) on the leaf of YN21 at 1dpi, and the new hyphae emerged at 2dpi (Fig. 1A e). At 3 dpi, hyphae were occasionally observed, and most asexual conidia failed to develop or form appressoria on MYC leaves (Fig. 1A c, enlarged as Fig. 1A g and Fig. 1A h). However, mycelium strewed the leaves of YN21 (Fig. 1A f). The biomass ratio experiment further validated that MYC was resistant, whereas YN21 was susceptible (Fig. 1B).

The F_1 progeny of YN21 and MYC all exhibited susceptibility to the *Bgt* isolate E09, mirroring the phenotype of YN21. In an F_2 population of 159 plants, 39 showed resistance symptoms (IT = 0–2), while 120 were susceptible to *Bgt* isolate E09 (IT = 3–4) [18, 22, 23]. The segregation ratio for resistance and susceptibility was 1:3 ($\chi^2 = 0.002$, $P = 0.963$). Additionally, the $F_{2:3}$ families segregated into 39 homozygous resistant, 79 segregating, and 40 homozygous susceptible plants, fitting the expected 1:2:1 ratio ($\chi 2 = 0.192$, $P = 0.906$), consistent with Mendelian inheritance controlled by a single recessive gene, temporarily designated as *PmMYC*.

Evaluation and alignment of sequencing data

After filtering low-quality reads and adaptor sequences, we obtained clean reads of 34,873,857 for MYC, 35,048,776 for YN21, 79,309,015 for resistant bulks, and 81,811,876 for susceptible bulks. Correspondingly, the clean data for MYC and YN21 were over 10 GB each, while the resistant and susceptible bulks were 23.719 GB and 24.474 GB, respectively. The Quality Score of 30, which indicates a 1 in 1000 probability of an incorrect base call, was above 94% for all libraries. The GC content

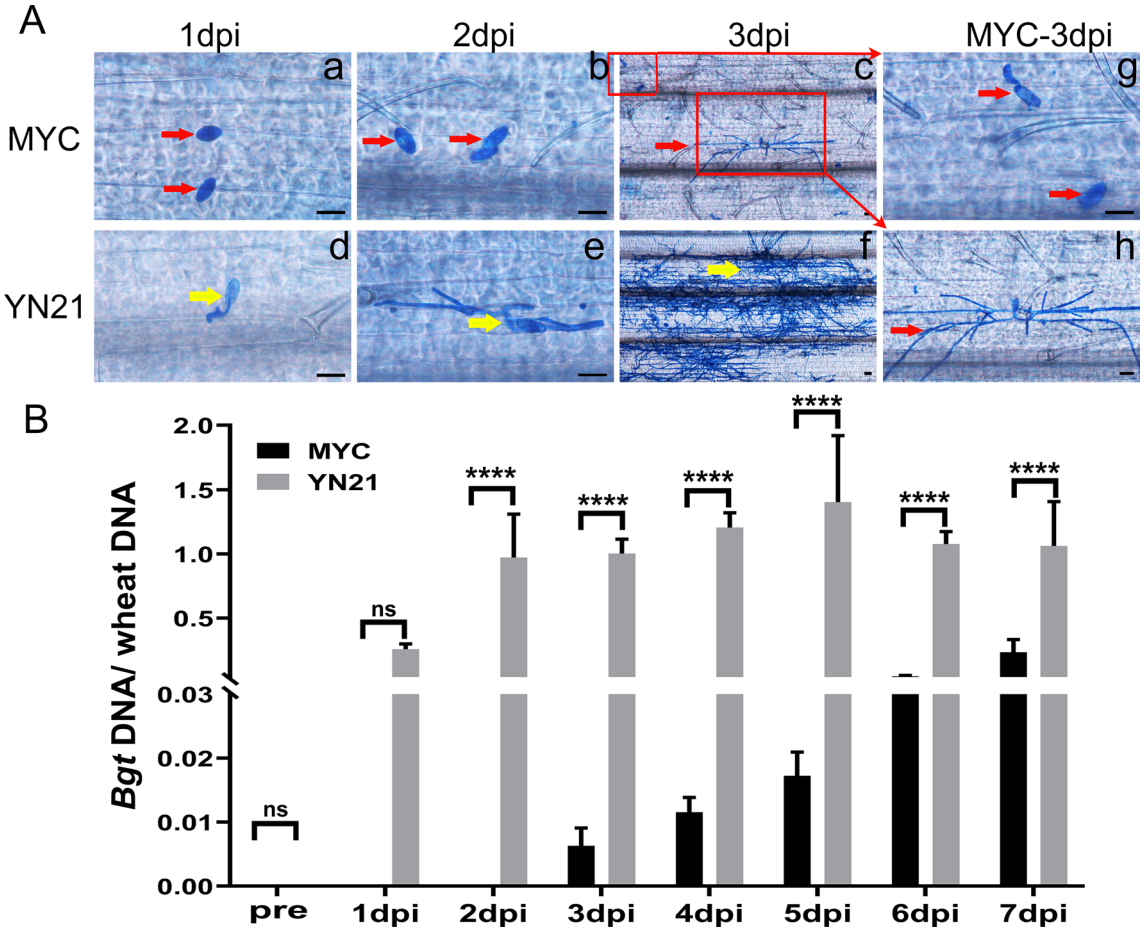

Fig. 1 Symptom development in resistant MYC and susceptible YN21 wheat cultivars. **(A)** Reactions of MYC and YN21 to *Blumeria graminis* f. sp. *tritici* (*Bgt*) isolate E09. Growth of *Bgt* isolate E09 was observed at 1, 2, and 3 dpi in the resistant cultivar MYC (a, b, c, g, h; red arrows) and the susceptible YN21 (d, e, f; yellow arrows). Images (g) and (h) showed the structure of *Bgt* in (c) under magnification. Scale bar: 100 μm. **(B)** Samples were collected at eight stages (pre-infection, 1dpi, 2 dpi, 3 dpi, 4 dpi, 5 dpi, 6 dpi, and 7 dpi) from the MYC and YN21 cultivars for biomass detection. "ns" indicates no significant difference; asterisks denote significant differences with **** representing $p < 0.0001$

ranged from 52.49 to 56.13%. The filtered clean reads were mapped to the reference genome (IWGSC RefSeq v2.1) using HISAT2 software (https://ccb.jhu.edu/software/hisat2/index.shtml) (Table S1). All subsequent analyses utilized these uniquely mapped reads. In summary, the data met the stringent requirements for subsequent SNP calling and DEGs analyses.

SNP calling and identification of candidate intervals

A total of 518,067 SNPs were identified, including 113,771 SNPs for MYC, 76,117 SNPs for YN21, 180,454 SNPs for the resistant bulks, and 147,725 SNPs for the susceptible bulks. Comparisons of MYC vs. YN21 and resistant vs. susceptible bulks revealed 40,650 and 52,222 SNPs, respectively. These SNPs might include ones that result from DNA mutations, RNA editing, or alternative splicing. Identical SNPs between the resistant bulks and the susceptible parent YN21 (44,113) were filtered out. Then, excluding SNPs with a support degree < 4 (58,061) and removing SNPs with consistent genotypes between the resistant and susceptible bulks (43,476), 14,058 high-quality and reliable SNPs were used for ED correlation and ΔSNP-index analysis.

Using ED correlation analysis, we identified 24 candidate intervals covering 139.39 Mb, distributed across the 2B and 2D chromosomes, and containing 1,131 genes (Fig. 2A, Table S2). In the ΔSNP-index correlation analysis, only six candidate intervals were identified on the 2BS chromosome near the centromere, with no candidate regions found on the 2D chromosome. The intersection of ED correlation and ΔSNP-index correlation analyses identified candidate intervals on the 2B chromosome, spanning a total length of 68.84 Mb and containing 743 annotated genes, which were determined to be the candidate regions for *PmMYC* (Fig. 2B, Table S3).

BLAST [34] was utilized to annotate the coding genes in these candidate intervals across multiple databases, including NR [35], Swiss-Prot [36], GO [24], KEGG [27], and COG [25, 26]. Consequently, 740 genes were annotated within these intervals. These genes were proposed as potential candidate loci for *PmMYC*, contributing to wheat powdery mildew resistance (Fig. 2C).

Analysis of DEGs

Among the samples, 17,965 differentially expressed genes (DEGs) were identified across MYC, YN21, and their progeny bulks inoculated with the *Bgt* E09 isolate. These gene expression profiles were shown in Fig. 3A. Among them, 12,175 DEGs were found between MYC and YN21, with 6,007 downregulated and 6,168 upregulated

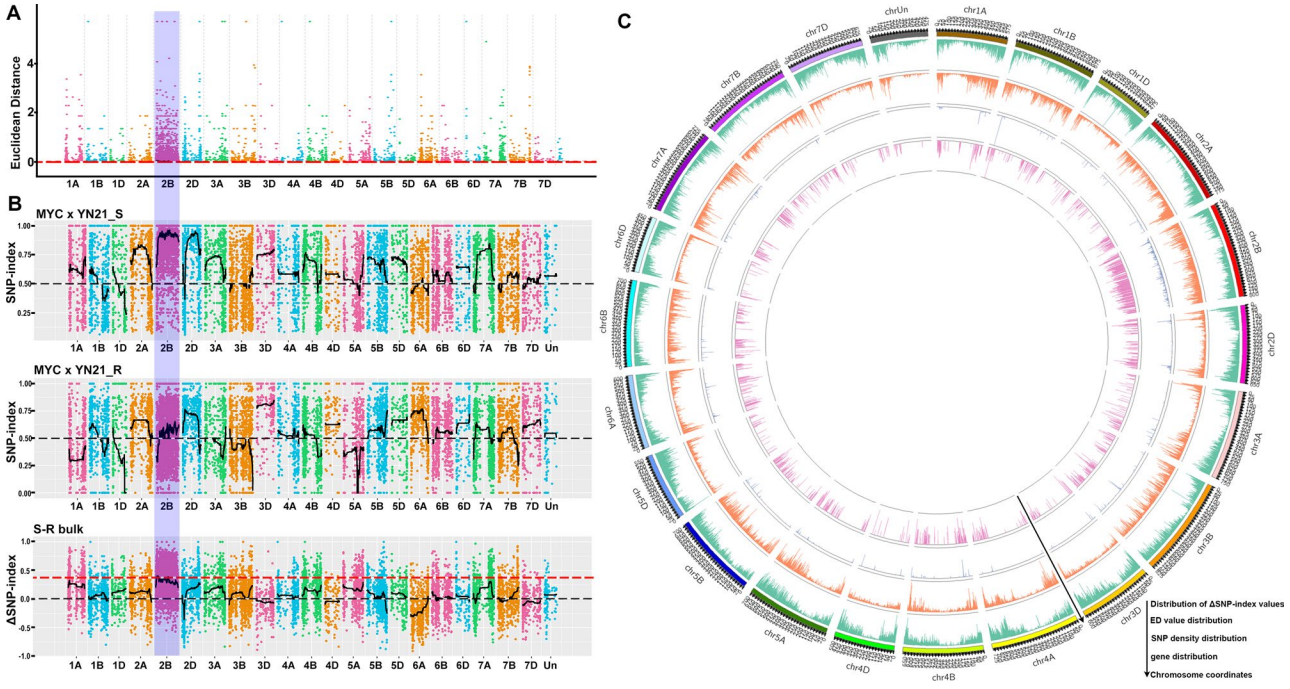

Fig. 2 Association analysis of SNPs. **(A)** Correlation analysis using the Euclidean Distance algorithm. The BSA location results were based on ED association. The X-axis showed the positions of the 21 wheat chromosomes, and the Y-axis represented the ED. Colored dots indicated the ED value of each SNP, the black line showed the fitted ED value, and the red dotted line represented the significance threshold. **(B)** Correlation results from the SNP-index method. The X-axis showed the positions of the 21 wheat chromosomes, and the Y-axis displayed the Δ (SNP-index). Colored dots displayed the calculated Δ(SNP-index) values. Black dotted lines indicated the fitted Δ (SNP-index) values and the red dotted line represented the significance threshold. **(C)** Visualization of results on the chromosomes. From the outside to the inside: chromosome coordinates, gene distribution, SNP density, ED value distribution, and Δ SNP-index value distribution

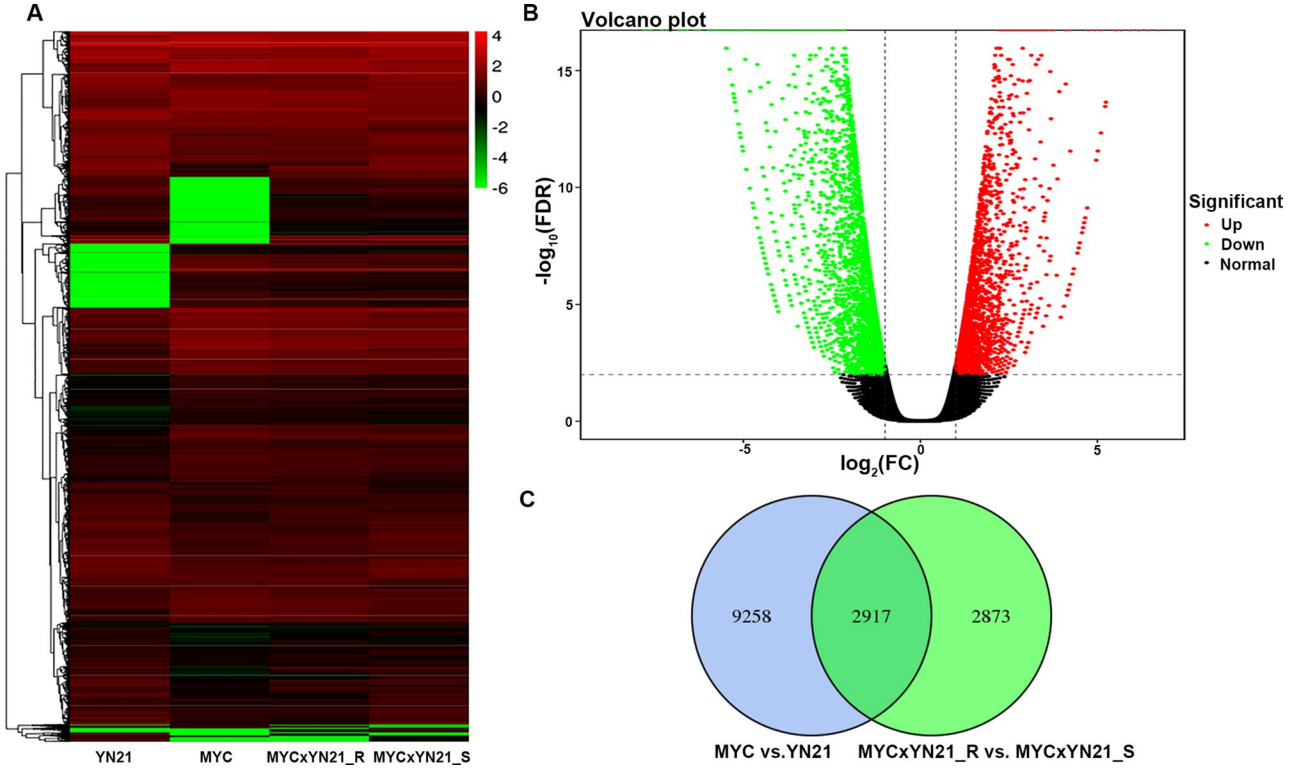

Fig. 3 DEGs annotations and analysis. **(A)** The analysis of all DEGs via BSR-seq from the parents and resistant and susceptible bulks. **(B)** Volcano plot of DEGs between the resistant parent MYC and the susceptible parent YN21. **(C)** The Venn diagram of DEGs between resistant and susceptible parents and bulks

(Fig. 3B). Additionally, 5,790 DEGs were detected in the resistant and susceptible bulks, with 3,290 downregulated and 2,500 upregulated. In the comparison of DEGs between parental lines and bulks, 9,258 DEGs exhibited unique expression patterns in the parents, while 2,873 DEGs demonstrated distinct expression profiles in bulks. Additionally, 2,917 DEGs displayed consistent expression patterns (Fig. 3C).

Alternative splicing events occurred following infection by powdery mildew

The primary types of alternative splicing include skip exon (SKIP), intron retention (IR), alternative exon ends (AE), alternative transcription start site (TSS), and alternative transcription terminal site (TTS) (Fig. 4A). Utilizing ASprofile software vision b-1.0.4 [29], we categorized these alternative splicing types into twelve distinct categories (Fig. 4B). Our analysis revealed that a significant number of alternative splicing events occurred in MYC, YN21, as well as the corresponding resistant and susceptible bulks after infection with *Bgt* isolate E09. Among these splicing events, TSS and TTS events occurrences were particularly prevalent, especially in the resistant bulks. Notably, key incidents of alternative splicing, specifically IR variants such as IR, MIR, XIR, and XMIR, were found to be more abundant in the resistant bulks.

TaSR34 (*TraesCS2D02G112200* and its homolog *TraesCS2A02G111600*), which encodes a serine/arginine-rich proteins involved in splicing regulation, exhibited both TTS and TSS splicing exclusively in the infected YN21; no such events were detected for these genes across other BSR samples.

Furthermore, *TaSF1* (*TraesCS2D02G281200*), encoding splicing factor 1 responsive to abscisic acid (ABA) and salicylic acid (SA), also produced TSS and TTS splice variants solely identified in infected YN21. AtPRP18a plays a role in pre-mRNA processing; loss-of-function mutations lead to intron retention phenomena. Its homolog *TraesCS2A02G197100* was shown to undergo exclusive TSS and TTS splicing only when YN21 was infected by *Bgt* (Supplemental table S7). These findings indicate that large-scale alternative splicing events have been uncovered through bulked segregant RNA sequencing across all samples subjected to *Bgt* infection.

The Venn diagram presented in Fig. 4C illustrates the alternative splicing events identified through BSA-seq in MYC, YN21, and the resistant and susceptible bulks infected by *Bgt*. A total of 36,146 AS events were shared among all four materials. Specifically, 670 AS events were detected in the resistant samples, while 444 AS events were identified in the susceptible samples. Furthermore,

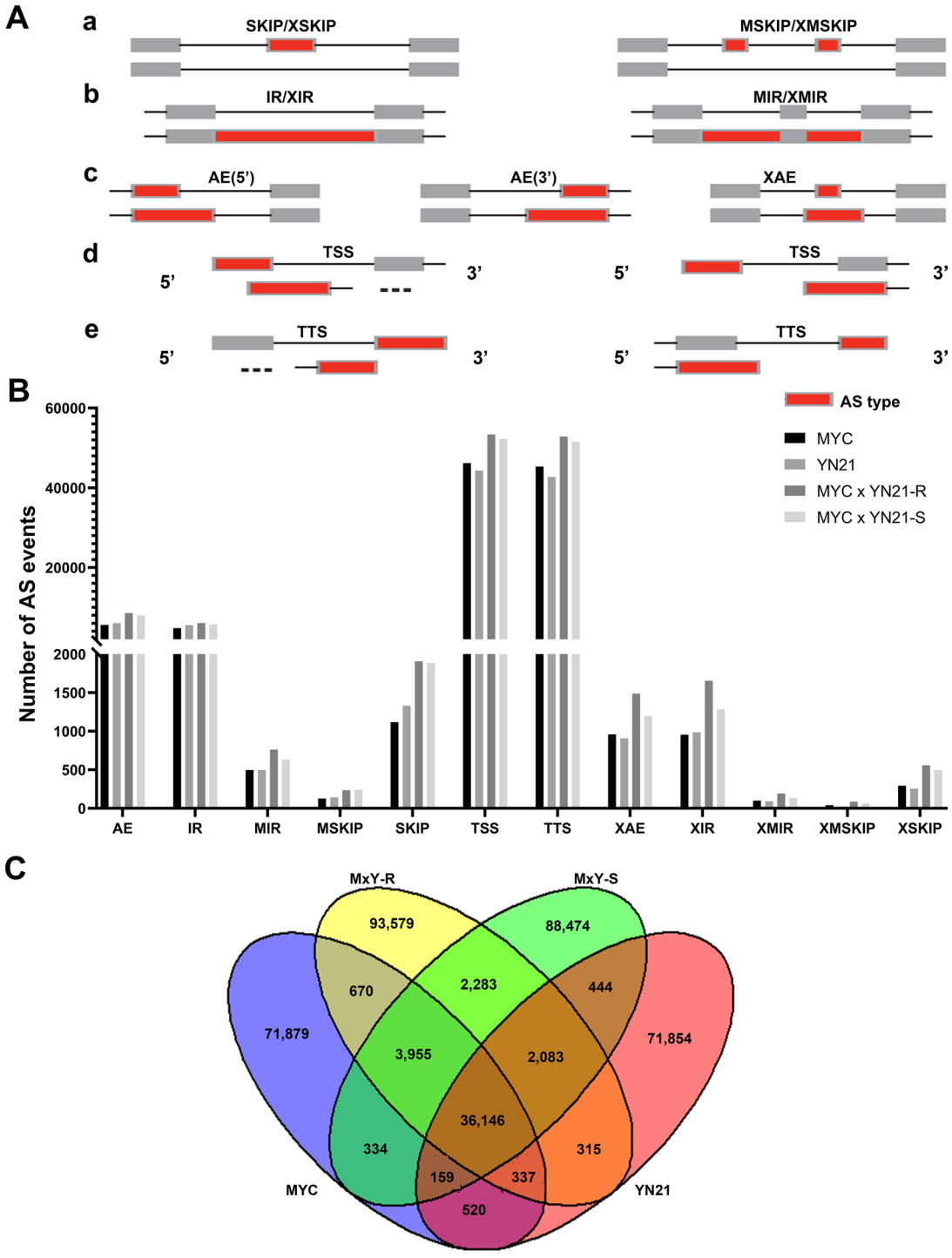

Fig. 4 Types of alternative splicing and number of alternative splicing events. **(A)** Schematic representation of alternative splicing types: (a) Exon skipping and multiple exon skipping; (b) Single intron retention and multiple intron retention; (c) Alternative exon; (d) Alternative transcription start site; (e) Alternative transcription termination site. The red rectangle highlights the alternative splicing type. **(B)** The column graph illustrates the types and number of alternative splicing events in MYC, YN21, along with resistant and susceptible bulks based on BSR-seq data. AE denotes Alternative exon ends; IR refers to intron retention; MIR signifies Multiple intron retention; MSKIP stands for Multiple exon skipping; SKIP represents exon skipping; TSS is Transcription start site; TTS is Transcription terminal site; XAE indicates Approximate alternative exon ends; XIR signifies Approximate intron retention; XMIR stands for Approximate multiple intron retention; XMSKIP represents Approximate multiple exon skipping; XSKIP denotes Approximate exon skipping. **(C)** The Venn diagram presents the alternative splicing events identified through BSA-seq in MYC and YN21 parents alongside resistant and susceptible bulks infected by *Bgt*. A total of 36,146 AS events were shared among all four samples. The unique AS events of MYC and YN21was recorded as 71,879 and 71,854 respectively

MYC and YN21 exhibited a remarkable number of unique AS events: 71,879 and 71,854 respectively.

Real-time PCR of the different expression genes

To investigate the role of DEGs in disease resistance, the relative expression levels of DEGs were measured at various time points (0, 3, 6, 12, 24, 36, 48, 72) hpi, corresponding to different developmental stages of *Bgt* E09 on susceptible wheat leaves: spore germination (0 hpi), primary germ tube formation (3 hpi), appressorium formation (6 hpi), penetration (12 hpi), and haustorium formation (24 hpi). In the GO enrichment analysis of all DEGs, a subset of 78 genes was identified as being involved in plant immune system processes. To identify resistance genes, twelve genes were selected from the pool of 78 defense-related differentially expressed genes based on their annotation for RT-PCR analysis. *TraesCS2B02G100300* and *TraesCS2B02G084000* encode the serine/threonine kinases with ATP binding activity. In the resistant parent MYC, their expression was detected before *Bgt* infection and increased gradually with *Bgt* invasion, peaking between 24 and 48 hpi, before decreasing. *TracesCS2B02G100300* was not expressed in the susceptible parent YN21, while *TracesCS2B02G084000* was expressed at low levels before and after inoculation with *Bgt* E09 in YN21 (Fig. 5A and B). These results suggested that *TraesCS2B02G100300* and *TraesCS2B02G084000* played roles in the early stage of *Bgt* infection, potentially inhibiting haustorium formation or secondary penetration. *TraesCS2B02G082200* and *TraesCS2B02G081900* encode kinases with ATP binding activity. In MYC, the expression of these genes gradually increased, peaking at

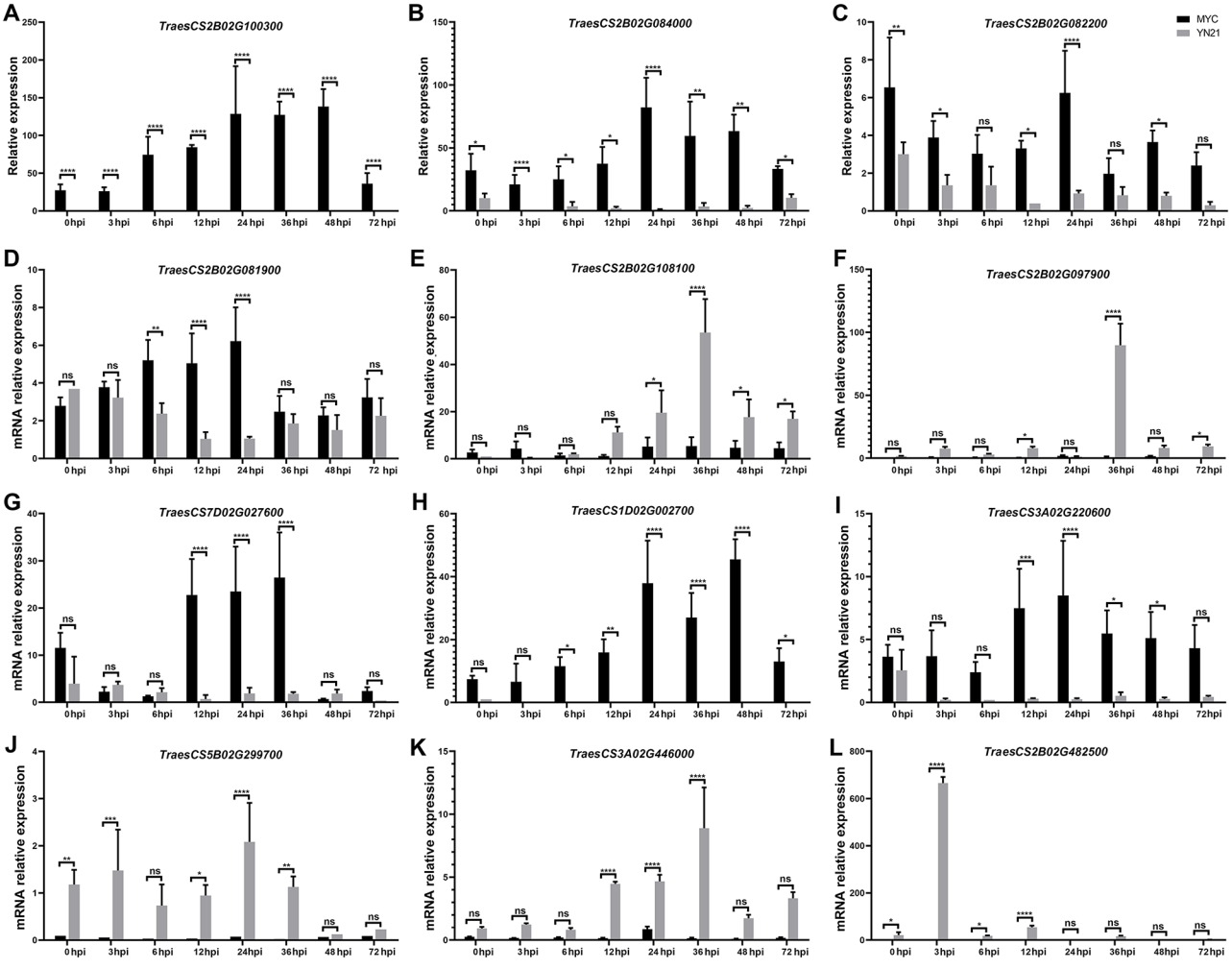

Fig. 5 Validation of the expression profile of DEGs in YN21 and MYC by real-time PCR. The expression profiles of 12 DEGs were validated by real-time PCR in the resistant parent MYC and the susceptible parent YN21, infected with *Bgt* isolate E09 at various stages: before inoculation, 3 hpi, 6 hpi, 12 hpi, 24 hpi, 36 hpi, 48 hpi, and 72 hpi. The x-axis represented the time of *Bgt* inoculation (hpi), and the y-xis represented the mRNA relative expression levels. The graphs presented DEG expression levels relative to β-tubulin, which served as the reference control. Data represent mean values with standard deviations from three independent experiments. "ns" indicates no significant difference, asterisks denote significant difference, *represents $p < 0.05$, ** represents $p < 0.01$, ***represents $p < 0.005$, and **** represents $p < 0.0001$

48 hpi before decreasing. In YN21, the expression of these genes showed a significant decline, reaching the lowest level at 24 hpi, followed by a gradual increase (Fig. 5C and D). *TracesCS2B02G082200* and *TracesCS2B02G081900* kinases were crucial for defending against *Bgt* invasion during the early stages. *TraesCS2B02G108100* encodes the F-box-like protein. The MLO (mildew resistance locus O)-like protein encoded by *TraesCS2B02G097900* is a heptahelical plasma membrane-localized protein that functions as a host factor required for *Bgt* invasion [37]. In YN21, the expression levels of these genes increased with *Bgt* infection, peaking at 36 hpi, whereas low-level expression was observed in MYC (Fig. 5E and F). These two proteins might play roles in the invasion process of *Bgt* isolate. *TraesCS7D02G027600* encodes a cell membrane integrin, *TraesCS1D02G002700* encodes an ATP-binding protein kinase, and *TraesCS3A02G220600* encodes a potential autophagy-related protein. In MYC, the expression of these genes peaked at 12–36, 24–48, and 12–24 hpi, respectively, before gradually declining. In contrast, extremely low or no expression was observed in YN21 (Fig. 5G and H, and Fig. 5I). These proteins might act as positive regulators of resistance to powdery mildew. *TraesCS5B02G299700* encodes an arginine succinate lyase, which is involved in amino acid transport and metabolism. *TraesCS3A02G446000* encodes a putative LRR receptor-like serine/threonine protein kinase [11]. *TraesCS2B02G482500* is associated with cold stress. These three genes were either not expressed or expressed at low levels in MYC. In YN21, *TraesCS2B02G482500* was specifically expressed at 3 hpi. *TraesCS5B02G299700* showed minimal expression variation from 0 to 36 hpi, whereas *TraesCS3A02G446000* expression increased with *Bgt* infection, peaking at 36 dpi (Fig. 5J and K, and Fig. 5L). These genes might be involved in the *Bgt* invasion process and function as negative regulators of the immune response.

GO analysis of all DEGs

To investigate the potential roles of DEGs in resistant and susceptible parental lines, we conducted a comprehensive GO analysis encompassing three primary categories: biological processes, molecular functions, and cellular components. Our findings revealed significant disparities in the expression profiles of DEGs compared to all genes (Fig. 6A), highlighting the key processes activated following *Bgt* infection. Notably, terms such as "response to stimuli" and "immune system process" were significantly enriched within the category of "biological processes", while "antioxidant activity" and "signal transducer activity" were predominantly identified in the "molecular function" category. These results underscore the distinct molecular mechanisms underlying resistance and susceptibility to powdery mildew.

COGs classification and KEGG pathway enrichment of DEGs within the *PmMYC* candidate intervals

The proteins encoded by 740 DEGs within the candidate intervals of *PmMYC* were classified using the COG database. The analysis revealed that these DEGs were primarily involved in transcription (9.76%), DNA replication, recombination, and repair (9.27%), as well as signal transduction processes (10.24%) (Fig. 6B). Additionally, they made significant contributions to general metabolic functions, accounting for 16.83%. Notably, seven of these DEGs were identified as being directly or indirectly associated with plant defense mechanisms, representing 1.71% of the total DEGs analyzed. These findings indicate that proteins related to the global stress response to powdery mildew encompass those involved in DNA transcription, replication, repair, recombination, and signal transduction (Fig. 6B).

We conducted KEGG pathway enrichment analysis for the same set of 740 DEGs within the candidate intervals (Fig. 6C). Two pathways emerged prominently: the plant-pathogen interaction pathway concerning powdery mildew (Fig. S2) and the disease-related MAPK cascade signaling pathway. These pathways suggest that the DEGs may play critical roles in responses to wheat powdery mildew.

SNP analysis within the *PmMYC* candidate intervals

We analyzed SNP mutation types in 740 genes within the candidate intervals identified by ED correlation and the ΔSNP-index method. The enrichment analysis of variant functional classes revealed that the dominant types were primarily synonymous coding, non-synonymous coding, intronic, and other variants. Compared to the parental lines, non-synonymous coding SNPs, intronic regions, upstream sequences, and other categories in bulks significantly increased (Fig. 7A).

We found 312 SNPs in the candidate intervals between the parental lines, including 70 non-synonymous mutations. Among the 443 SNPs found in resistant versus susceptible bulks, 99 were non-synonymous mutations. We further analyzed 169 non-synonymous coding SNPs within the candidate intervals. In our comparison across parental lines and bulks regarding non-synonymous coding SNPs within the candidate intervals: we found that 18 SNPs were unique to parents; 47 SNPs were unique to the bulks; while an additional 52 SNPs were present in both parents and bulks (Fig. S3). Mapping these 169 SNPs into the genome revealed that only 59 were mapped in the coding regions of candidate genes, corresponding to 46 potential genes. These 46 genes, with point mutations in MYC, were considered candidates for *PmMYC*. Additionally, only 13 of the 46 candidate genes exhibited significant differential expression between the resistant and susceptible parents and bulks (Fig. 7B).

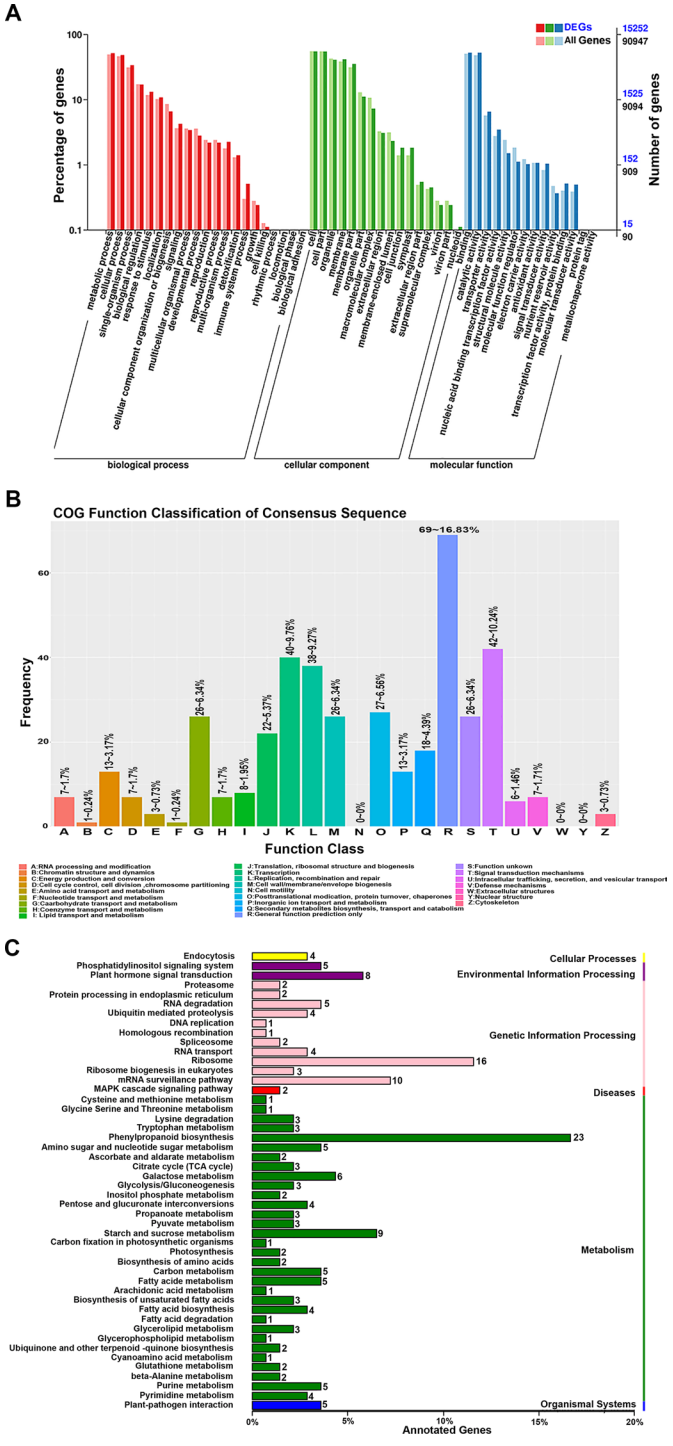

Fig. 6 GO analysis, COGs functional classification and KEGG pathway enrichment of DEGs. **(A)** GO enrichment analysis of DEGs and all genes. **(B)** COGs functional classification of DEGs in *PmMYC* candidate intervals. **(C)** KEGG pathway enrichment of DEGs distributed in *PmMYC* candidate regions

According to Fig. 7B result, *TraesCS2B02G131200*, *TraesCS2B02G076200*, *TraesCS2B02G132900*, and *TraesCS2B02G135800* were randomly selected from seven genes demonstrating distinct expression patterns between resistant and susceptible parents/bulks. These genes showed consistent expression patterns within the resistant parents and bulks, as well as within the susceptible parents and bulks (Fig. 7B). *TraesCS2B02G076200*, which encodes a protein from the Tetratricopeptide Repeat (TPR)-like superfamily, exhibited a fluctuating expression pattern from 0 to 72hpi in both MYC and YN21, peaking at 24 hpi before declining. Notably, its

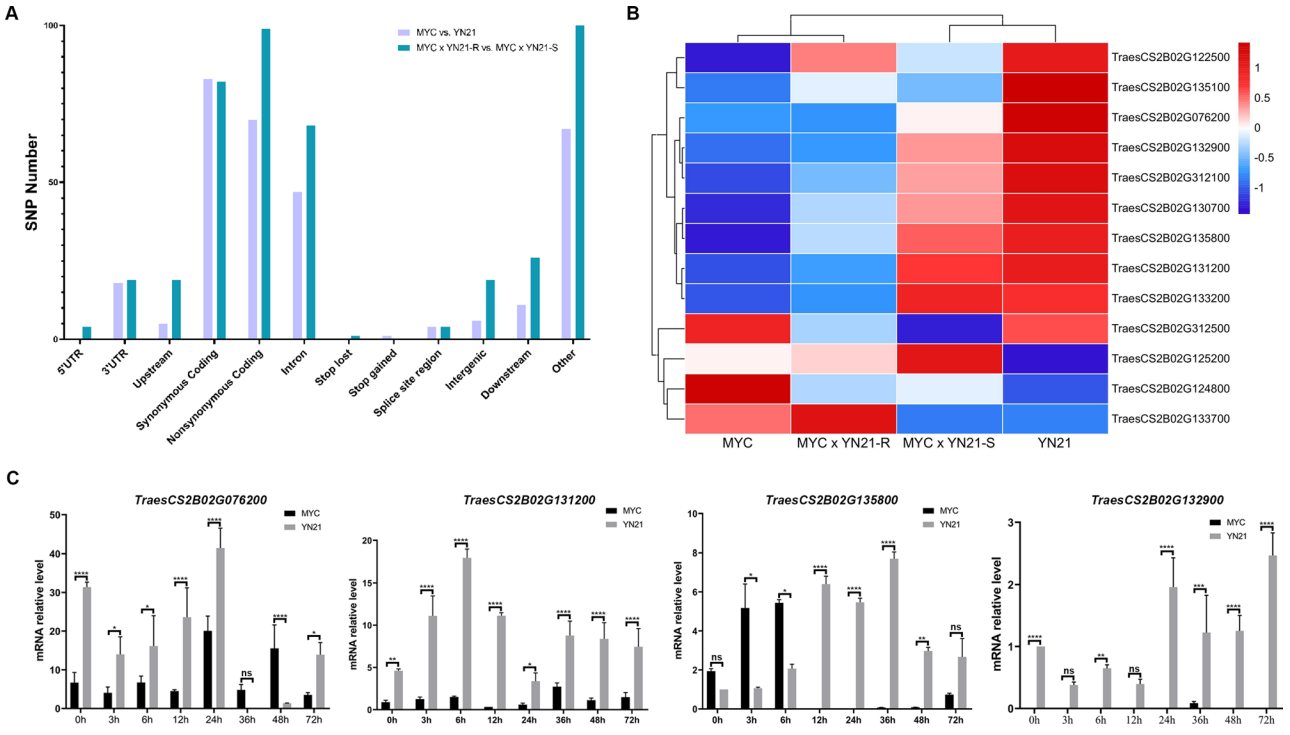

Fig. 7 Analysis of non-synonymous SNPs within candidate intervals potentially identifying *PmMYC*. **(A)** Statistical analysis of SNP types and the number of non-synonymous mutations within candidate intervals. **(B)** Thirteen genes with non-synonymous SNP variants in candidate intervals showed significant differential expression between resistant and susceptible parents and bulks. **(C)** The expression profiles of four DEGs within candidate intervals were validated by real-time PCR before and after infection with *Bgt* isolate E09, at 3 hpi, 6 hpi, 12 hpi, 24 hpi, 36 hpi, 48 hpi, and 72 hpi in the resistant MYC and the susceptible YN21. β-tubulin served as the reference control. Data were presented as means ± SD from three experiments. "ns" indicates no significant difference, asterisks stand for significant difference, *represents $p < 0.05$, ** represents $p < 0.01$, ***represents $p < 0.005$, and **** represents $p < 0.0001$

expression was significantly lower in MYC than in YN21 at all stages following *Bgt* inoculation (Fig. 7C). *TraesCS2B02G135800* encodes a CW-type zinc finger protein. Its expression was significantly higher in MYC compared to YN21 from 0 to 6hpi. After this period, expression increased in YN21 but was suppressed in MYC (Fig. 7C). *TraesCS2B02G131200* encodes an adenine nucleotide alpha hydrolases-like protein. Its expression initially rose and then declined, peaking at 6 hpi, with levels considerably higher in YN21 (Fig. 7C). *TraesCS2B02G132900* encodes an AAA-type ATPase family protein. It exhibited a fluctuating expression pattern, with peaks at 24 hpi and 72 hpi in YN21, while showing minimal expression in MYC (Fig. 7C). Based on the temporal expression profiles of *TraesCS2B02G131200*, *TraesCS2B02G076200*, *TraesCS2B02G132900*, and *TraesCS2B02G135800* following *Bgt* invasion, these genes exhibited distinct expression patterns between the resistant MYC and the susceptible YN21 cultivars (Fig. 7C). *TraesCS2B02G131200*, *TraesCS2B02G076200*, and *TraesCS2B02G132900* are potentially sensitivity-related genes whose expression was suppressed in MYC, which likely contributes to its observed resistance to powdery mildew. In contrast, these genes were expressed at higher levels in YN21, suggesting a potential mechanism through which MYC combats *Bgt* infection.

Discussion

The *PmMYC* candidate narrowed within 46 genes

Bulked Segregant RNA-sequencing integrates bulked segregant analysis with RNA-sequencing, providing a powerful method for exploring complex polyploid genomics. Using BSR-Seq, *PmMYC* was mapped to the physical intervals 40,451,950−102,426,703 bp and 421,707,046–449,840,516 bp on Chromosome 2B. These candidate genomic regions encompassed a total of 740 genes, potentially including *PmMYC*. Notably, the candidate intervals for *PmMYC* do not overlap with those previously identified for *PmYD588*. The latter was discovered in the Chinese wheat breeding line YD588, which demonstrates high resistance to powdery mildew at both seedling and adult stages. Through BSR-Seq combined with SNP association analysis, *PmYD588* was mapped to a precise interval of 4.2 cM on chromosome arm 2B. This locus holds significant promise for breeding powdery mildew-resistant wheat cultivars [18]. The *PmMYC* locus is located on the long arm of chromosome 2B near the centromere and is distinct from other known resistance

loci such as *Pm52*, *Pm6*, *Pm63*, *Pm64*, *Pm51*, and *Pm33* found at the distal end of chromosome arm 2BL [38].

Among all types of SNPs, non-synonymous mutations altered the properties of the encoded amino acids, leading to changes in protein function. The non-synonymous mutation in *PmMYC* conferred resistance to powdery mildew in MYC but caused susceptibility in YN21. We identified and characterized 169 non-synonymous mutations, narrowing them down to 46 candidate genes, among which 13 displayed differential expression profiles and impacted protein function. Notably, most of these 13 genes were down-regulated in MYC, aligning with real-time PCR validation. While these 13 genes will be further explored as potential candidates for *PmMYC* resistance, it was also important to consider that non-synonymous mutations could influence protein function without altering mRNA levels. Thus, all 46 genes remained relevant candidates for understanding the role of *PmMYC* in modulating resistance to *Bgt*. This comprehensive analysis underscored the complex regulatory role of *PmMYC* in defense mechanisms and highlighted the need for further investigation to elucidate its exact function in resistance.

The alteration of alternative splicing may represent a tactic utilized by *Bgt* during its infection in wheat

Exons of precursor mRNA (pre-mRNA) produced during gene transcription can undergo alternative splicing, resulting in a diverse array of mature mRNA isoforms and proteins. This process enhanced biological diversity by allowing genes to generate distinct transcripts and proteins, each serving specific molecular functions.

In animals, alternative splicing was well-documented to be regulated by various extracellular stimuli [39]. However, in plants, the molecular mechanisms driving the widespread changes in alternative splicing during pathogen invasion remained poorly understood. Huang et al. (2020) identified global alterations in alternative splicing during mRNA maturation in tomato leaves infected with *Phytophthora infestans* [40]. They found approximately 2,000 genes exhibiting specific alternative splicing patterns, with minimal changes in overall gene expression levels [40]. These findings suggested that alternative splicing significantly reshaped the plant transcriptome in response to pathogen interactions.

P. infestans appeared to manipulate alternative splicing machinery to disrupt host immunity. Gui et al. (2022) further elucidated this by demonstrating that the effector protein PSR1 (*Phytophthora* suppressor factor 1) of *Phytophthora infestans* hijacked the host's pre-mRNA splicing machine to regulate small RNA biogenesis and impair plant immunity [41]. PSR1 interacting protein 1 (PINP1) specifically bound PSR1 through its three conserved C-terminal domains. PINP1 exhibited RNA binding and helicase activities, inhibiting RNA metabolism and small RNA production, which resulted in widespread alteration in alternative splicing.

Our experiments suggest that upon invasion by *Bgt*, the pathogen reprograms the plant transcriptome by modifying or inactivating splicing factors and auxiliary components of plant splicing machinery. The genes *TaSR34* (*TraesCS2D02G112200* and its homolog *TraesCS2A02G111600*), *TraesCS2A02G197100* (a homolog of AtPRP18a), and *TaSF1* (*TraesCS2D02G281200*) underwent TTS and TSS splicing events that were exclusively observed in YN21 infected with *Bgt*. All proteins encoded by these genes are implicated in alternative pre-mRNA splicing and must affect mRNA maturation and function of protein products. Following invasion by *Bgt* may involve a multi-layered strategy aimed at detecting vulnerabilities within the wheat immune system; once these weaknesses are discerned by pathogens they can penetrate deeply to effectively paralyze this defense mechanism. We hypothesize that *Bgt* targets alternative splicing machinery as part of its attack strategy, modifying or altering its components or auxiliary factors to reprogram the plant transcriptome and regulate the expression of immune-related genes.

The KEGG pathway enrichment analysis of DEGs in candidate regions supported this hypothesis by highlighting significant involvement in RNA metabolism and mRNA surveillance. These findings suggest that manipulation of the splicing machinery may serve as a crucial strategy employed during pathogen infection. Investigating the underlying molecular mechanisms could significantly enhance the discovery of broad-spectrum resistance genes and facilitate the development of disease-resistant crops.

Conclusion

Our study demonstrated that the wheat genotype MYC possessed robust resistance to *Bgt*, attributed to the recessive gene *PmMYC*. The integration of BSR-Seq and genetic analyses identified critical genomic regions and potential candidate genes linked to this resistance. *PmMYC* represents a novel gene conferring resistance to powdery mildew. Our findings suggested that *PmMYC* might function as a negative regulator of resistance to *Bgt* invasion. Differentially expressed genes enriched in immune-related pathways highlighted the complex defense mechanisms at play. These findings advanced our understanding of the immune response to wheat powdery mildew and provided valuable insights for breeding durable-resistant cultivars.

Abbreviations

Bgt	*Blumeria graminis* f. sp. *Tritici*
PAMP	Pathogen-associated molecular pattern
PTI	PAMP-triggered immunity

ETI	Effector-triggered immunity
PRRs	Pattern recognition receptors
NLRs	Nucleotide-binding domain and Leucine-rich repeat Receptors
HR	Hypersensitive reactions
R genes	Resistance genes
BSA	Bulked Segregant Analysis
BSR	Bulked Segregant Analysis (BSA) and RNA sequencing
YN21	Yannong21
dpi	Day post-inoculation
hpi	Hour post-inoculation
ITs	Infection types
InDel	Insertion/deletion
GO	Gene Ontology
COG	Cluster of Orthologous Groups
KEGG	Kyoto Encyclopedia of Genes and Genomes
ED	Euclidean distance
DEGs	Differently expression genes
FPKM	Fragments Per Kilobase of transcript per Million fragments mapped
FDR	Error detection rate
FC	Fold Change
IWGSC	International Wheat Genome Sequencing Consortium
AS	Alternative splicing
Q30	Quality Score of 30
AE	Alternative exon ends
IR	Intron retention
MIR	Multiple intron retention
MSKIP	Multiple exon skipping
SKIP	Exon skipping
TSS	Transcription start site
TTS	Transcription terminal site
XAE	Approximate alternative exon ends
XIR	Approximate intron retention
XMIR	Approximate multiple intron retention
XMSKIP	Approximate multiple exon skipping
XSKIP	Approximate exon skipping
pre-mRNA	Precursor mRNA
PSR1	*Phytophthora* suppressor factor 1
PINP1	PSR1 interacting protein 1

Supplementary Information

The online version contains supplementary material available at https://doi.org/10.1186/s12870-024-05789-9.

Supplementary Material 1: Table S1. Sequencing Data.

Supplementary Material 2: Table S2. SNP-associated region information (results from ED method).

Supplementary Material 3: Table S3. SNP Associated Region Information（results of ΔSNP-index methods).

Supplementary Material 4: Table S4. SNP annotation statistics in candidate regions.

Supplementary Material 5: Table S5. Primers used in this study.

Supplementary Material 6: Table S6. Raw data of enriched and annotated terms.

Supplementary Material 7: Table S7. Alternative splicing transcripts and types in MYC, YN21, as well as resistant and susceptible bulks.

Supplementary Material 8: Fig. S1 Development of symptoms corresponding to biomass timepoint series. Fig. S2 KEGG pathway enrichment of DEGs indicating involvement in plant-pathogen interactions in MYC. Differentially expressed proteins in the red box were enriched in the plant-pathogen pathway and were significantly upregulated in both resistant parents and bulks, contributing to the resistance response against powdery mildew. Fig. S3 Venn diagram illustrating non-synonymous coding SNPs within the PmMYC candidate intervals.

Author contributions
SC, YJ, CX, and RL participated in image acquisition and data analysis and prepared Figures. SC, BW, and TY engaged in data visualization. YL and TM Participated in the phenotypic analysis of powdery mildew. TY drafted and revised the manuscript. TY and PM supervise the project. All authors read and approved the final manuscript.

Funding
This work was supported by the National Natural Science Foundation of China 32072053 and the Natural Science Foundation of Shandong (ZR2022MC217).

Data availability
Sequence data that support the findings of this study have been deposited in the China Genome Sequence Archive with the primary accession code GSA: CRA018130 and the direct web link as the following: https://bigd.big.ac.cn/gsa/browse/CRA018130.

Declarations

Ethics approval and consent to participate
Not applicable.

Consent for publication
Not applicable.

Competing interests
The authors declare no competing interests.

Received: 28 July 2024 / Accepted: 6 November 2024
Published online: 11 November 2024

References

1. Singh RP, Singh PK, Rutkoski J, Hodson DP, He X, Jorgensen LN, et al. Disease Impact on Wheat Yield potential and prospects of genetic control. Annu Rev Phytopathol. 2016;54:303–22.
2. Jin Y, Han G, Zhang W, Bu B, Zhao Y, Wang J, et al. Evaluation and genetic dissection of the powdery mildew resistance in 558 wheat accessions. New Crops. 2024;1:100018.
3. Li L, Weigel D. One hundred years of Hybrid Necrosis: Hybrid Autoimmunity as a window into the mechanisms and Evolution of Plant-Pathogen interactions. Annu Rev Phytopathol. 2021;59:213–37.
4. Bourras S, Praz CR, Spanu PD, Keller B. Cereal powdery mildew effectors: a complex toolbox for an obligate pathogen. Curr Opin Microbiol. 2018;46:26–33.
5. Yu TY, Sun MK, Liang LK. Receptors in the induction of the Plant Innate Immunity. Mol Plant Microbe Interact. 2021;34(6):587–601.
6. An Y, Zhang M. Advances in understanding the plant-Ralstonia solanacearum interactions: unraveling the dynamics, mechanisms, and implications for crop disease resistance. New Crops. 2024;1:100014.
7. Boller T, Felix G. A Renaissance of elicitors: Perception of Microbe-Associated molecular patterns and Danger signals by pattern-recognition receptors. Annu Rev Plant Biol. 2009;60(60, 2009):379–406.
8. Yuan M, Jiang Z, Bi G, Nomura K, Liu M, Wang Y, et al. Pattern-recognition receptors are required for NLR-mediated plant immunity. Nature. 2021;592(7852):105–9.
9. Ngou BPM, Ahn H-K, Ding P, Jones JDG. Mutual potentiation of plant immunity by cell-surface and intracellular receptors. Nature. 2021;592(7852):110–5.
10. Feehan JM, Wang J, Sun X, Choi J, Ahn H-K, Ngou BPM, et al. Oligomerization of a plant helper NLR requires cell-surface and intracellular immune receptor activation. Proc Natl Acad Sci U S A. 2023;120(11):e2210406120.
11. Wei X, Liu X, Zhang X, Guo S, Shi J. Structural insights into ligand recognition and receptor activation of plant leucine-rich repeat (LRR) transmembrane receptors. New Crops. 2024;1:100022.
12. Gardiner L-J, Wingen LU, Bailey P, Joynson R, Brabbs T, Wright J, et al. Analysis of the recombination landscape of hexaploid bread wheat reveals genes controlling recombination and gene conversion frequency. Genome Biol. 2019;20(1):69.

13. Nieri D, Di Donato A, Ercolano MR. Analysis of tomato meiotic recombination profile reveals preferential chromosome positions for NB-LRR genes. Euphytica. 2017;213(9):206.
14. Petersen G, Seberg O, Yde M, Berthelsen K. Phylogenetic relationships of Triticum and Aegilops and evidence for the origin of the A, B, and D genomes of common wheat (Triticum aestivum). Mol Phylogenet Evol. 2006;39(1):70–82.
15. Bourras S, McNally KE, Ben-David R, Parlange F, Roffler S, Praz CR, et al. Multiple avirulence loci and Allele-Specific Effector Recognition Control the Pm3 race-specific resistance of wheat to Powdery Mildew. Plant Cell. 2015;27(10):2991–3012.
16. Stirnweis D, Milani SD, Brunner S, Herren G, Buchmann G, Peditto D, et al. Suppression among alleles encoding nucleotide-binding–leucine-rich repeat resistance proteins interferes with resistance in F1 hybrid and allele-pyramided wheat plants. Plant J. 2014;79(6):893–903.
17. Brunner S, Hurni S, Streckeisen P, Mayr G, Albrecht M, Yahiaoui N, et al. Intragenic allele pyramiding combines different specificities of wheat Pm3 resistance alleles. Plant J. 2010;64(3):433–45.
18. Ma P, Wu L, Xu Y, Xu H, Zhang X, Wang W, et al. Bulked segregant RNA-Seq provides distinctive expression Profile Against Powdery Mildew in the wheat genotype YD588. Front Plant Sci. 2021;12:764978.
19. Li M, Dong L, Li B, Wang Z, Xie J, Qiu D, et al. A CNL protein in wild emmer wheat confers powdery mildew resistance. New Phytol. 2020;228(3):1027–37.
20. Wang N, Tang C, Fan X, He M, Gan P, Zhang S, et al. Inactivation of a wheat protein kinase gene confers broad-spectrum resistance to rust fungi. Cell. 2022;185(16):2961–e29742919.
21. Ma P, Xu H, Luo Q, Qie Y, Zhou Y, Xu Y, et al. Inheritance and genetic mapping of a gene for seedling resistance to powdery mildew in wheat line X3986-2. Euphytica. 2014;200(1):149–57.
22. Liu Z, Sun Q, Ni Z, Yang T, McIntosh RA. Development of SCAR markers linked to the Pm21 gene conferring resistance to powdery mildew in common wheat. Plant Breeding. 1999;118(3):215–9.
23. He H, Guo R, Gao A, Chen Z, Liu R, Liu T, et al. Large-scale mutational analysis of wheat powdery mildew resistance gene Pm21. Front Plant Sci. 2022;13:988641.
24. Ashburner M, Ball CA, Blake JA, Botstein D, Butler H, Cherry JM, et al. Gene ontology: tool for the unification of biology. The Gene Ontology Consortium. Nat Genet. 2000;25(1):25–9.
25. Tatusov RL, Galperin MY, Natale DA, Koonin EV. The COG database: a tool for genome-scale analysis of protein functions and evolution. Nucleic Acids Res. 2000;28(1):33–6.
26. Tatusov RL, Koonin EV, Lipman DJ. A genomic perspective on protein families. Science. 1997;278(5338):631–7.
27. Kanehisa M, Goto S, Kawashima S, Okuno Y, Hattori M. The KEGG resource for deciphering the genome. Nucleic Acids Res. 2004;32(Database issue):D277–280.
28. McKenna A, Hanna M, Banks E, Sivachenko A, Cibulskis K, Kernytsky A, et al. The genome analysis Toolkit: a MapReduce framework for analyzing next-generation DNA sequencing data. Genome Res. 2010;20(9):1297–303.
29. Trapnell C, Williams BA, Pertea G, Mortazavi A, Kwan G, van Baren MJ, et al. Transcript assembly and quantification by RNA-Seq reveals unannotated transcripts and isoform switching during cell differentiation. Nat Biotechnol. 2010;28(5):511–5.
30. Abe A, Kosugi S, Yoshida K, Natsume S, Takagi H, Kanzaki H, et al. Genome sequencing reveals agronomically important loci in rice using MutMap. Nat Biotechnol. 2012;30(2):174–8.
31. Shannon P, Markiel A, Ozier O, Baliga NS, Wang JT, Ramage D, et al. Cytoscape: a software environment for integrated models of biomolecular interaction networks. Genome Res. 2003;13(11):2498–504.
32. Ghosh D. Incorporating the empirical null hypothesis into the Benjamini-Hochberg procedure. Stat Appl Genet Mol Biol 2012, 11(4).
33. Sherman BT, Hao M, Qiu J, Jiao X, Baseler MW, Lane HC, et al. DAVID: a web server for functional enrichment analysis and functional annotation of gene lists (2021 update). Nucleic Acids Res. 2022;50(W1):W216–21.
34. Altschul SF, Madden TL, Schäffer AA, Zhang J, Zhang Z, Miller W, et al. Gapped BLAST and PSI-BLAST: a new generation of protein database search programs. Nucleic Acids Res. 1997;25(17):3389–402.
35. Deng YY, Li JQ, Wu SF, Zhu Y, Chen YW, He FC. Integrated Nr Database in protein annotation system and its localization. Comput Eng. 2006;32:71–2.
36. Apweiler R, Bairoch A, Wu CH, Barker WC, Boeckmann B, Ferro S, et al. UniProt: the Universal protein knowledgebase. Nucleic Acids Res. 2004;32(suppl1):D115–9.
37. Panstruga R. Serpentine plant MLO proteins as entry portals for powdery mildew fungi. Biochem Soc Trans. 2005;33(Pt 2):389–92.
38. Wang B, Meng T, Xiao B, Yu T, Yue T, Jin Y, et al. Fighting wheat powdery mildew: from genes to fields. Theor Appl Genet. 2023;136(9):196.
39. Lee Y, Rio DC. Mechanisms and regulation of alternative Pre-mRNA splicing. Annu Rev Biochem. 2015;84:291–323.
40. Huang J, Lu X, Wu H, Xie Y, Peng Q, Gu L, et al. Phytophthora Effectors modulate genome-wide alternative splicing of host mRNAs to Reprogram Plant Immunity. Mol Plant. 2020;13(10):1470–84.
41. Gui X, Zhang P, Wang D, Ding Z, Wu X, Shi J, et al. Phytophthora effector PSR1 hijacks the host pre-mRNA splicing machinery to modulate small RNA biogenesis and plant immunity. Plant Cell. 2022;34(9):3443–59.
42. Takagi H, Abe A, Yoshida K, Kosugi S, Natsume S, Mitsuoka C, et al. QTL-seq: rapid mapping of quantitative trait loci in rice by whole genome resequencing of DNA from two bulked populations Summary. Plant J 2013:74 (1) 174–183. https://doi.org/10.1111/tpj.12105

Publisher's note